DEMONSTRATION OF ENGINEERED MULTI-LAYERED SIC-SIC CLADDING WITH ENHANCED ACCIDENT TOLERANCE

C.P. DECK, H.E. KHALIFA, G. JACOBSEN, J. SHEEDER, K. SHAPOVALOV, S. GONDERMAN, E. SONG, J. GAZZA, C.A. BACK
Nuclear Technologies and Materials Division, General Atomics
P.O. Box 85608, San Diego, CA 92186-5608 - USA

P. XU, F. BOYLAN, R. JACKO
Westinghouse Electric Company LLC
1332 Beulah Road, Pittsburgh, PA 15235 - USA

ABSTRACT

Engineered cladding consisting of layers of monolithic silicon carbide (SiC) and SiC fiber reinforced SiC matrix (SiC-SiC) composite has potential to offer significant performance benefits and enhanced accident tolerance compared to existing light water reactor fuel rod designs. General Atomics is developing a multi-layered cladding design that offers toughness, hermeticity, stability under irradiation, and retention of strength and performance at high temperatures and in potential accident conditions.

Recent progress has focused on both the fabrication and characterization of this enhanced accident tolerant fuel cladding. Fabrication efforts have addressed scale-up in cladding length while meeting demanding dimensional tolerances and surface roughness requirements. In addition, a robust, SiC-based joining and sealing process has been demonstrated which is capable of fabricating cladding samples containing a pressurized gas backfill necessary for fuel rod applications. Mechanical and thermal properties including strength and thermal conductivity have been measured over a range of temperatures corresponding to normal operation and accident conditions. The hermeticity of the engineered cladding (including the tube and end plug joints) has been measured using high sensitivity helium leak detection. Cladding corrosion performance has been measured out-of-pile (in flowing loop autoclaves under pressurized water reactor chemistry conditions), and sealed cladding samples retained hermeticity and showed extremely low corrosion mass loss.

1. Introduction

There is significant interest in nuclear fuel and cladding which can offer enhanced accident tolerance and improved economics to support the current fleet of light water reactors. Silicon carbide (SiC) materials, in both monolithic and silicon carbide fiber reinforced, silicon carbide matrix (SiC-SiC) composite form are being actively developed for use in accident tolerant fuel (ATF) cladding applications [1]. In this cladding application, the ability of silicon carbide to retain strength and geometry at high temperatures, and the stable behavior and swelling under irradiation [2] make it appealing in both normal operation and accident conditions.

In order to meet cladding performance requirements, an engineered, multi-layered cladding structure, consisting of tough composite layers and dense, hermetic and corrosion resistant monolithic SiC layers has been developed. Fabrication and demonstration efforts on SiC-based cladding have been ongoing at General Atomics since 2009, and progress in fabrication and joining [3], characterization [4], and modeling [5] has led to the development of SiGA[tm] [1] silicon carbide cladding technology for accident tolerant fuel. This development program is ongoing, with concurrent efforts focusing on improvement of cladding performance, fabrication

[1] SiGA[tm] is a trademark of General Atomics.

yield and scale-up of manufacturing capabilities, and irradiation testing to support future licensing and commercialization efforts.

In this work, recent results on mechanical, thermal, leak tightness, and corrosion performance are presented. High temperature mechanical testing was performed to examine retention of strength and coolable geometry in potential LOCA accident scenarios. High thermal conductivity values were measured for as-fabricated SiC-based cladding, and can be controlled by processing and final cladding density and structure. Testing of hermeticity showed manufacturing process control that can reliably produce hermetic cladding tubes and joints with high yield. Corrosion testing revealed that sealed corrosion samples made using carefully controlled fabrication conditions can meet demanding corrosion specifications under autoclave testing. Together, these represent key properties that contribute to the overall behavior of SiGA cladding that make this extremely promising for use in ATF applications.

2. Experimental Methods

2.1. Fabrication

In this work, SiC-based cladding with an engineered, multi-layered structure was fabricated and characterized. This structure consists of an outer monolithic CVD SiC layer over an inner fiber reinforced SiC-SiC composite layer. Near-stoichiometric SiC fiber (Hi-Nicalon type-S fiber, NGS Advanced Fiber Co.) was used as the reinforcing fiber, and after preforming this fiber into tubular geometries, chemical vapor infiltration (CVI) was used to densify the composite. The CVI process used had two main steps, with an initial process used to form a pyrolytic carbon interphase coating on the fibers followed by depositing a high purity, stoichiometric SiC matrix. A monolithic SiC coating was then applied using a chemical vapor deposition (CVD) process. Surface roughness specifications were met using a centerless grinder. The fabrication process described above reliably and repeatedly produced cladding tube samples with inner diameters of ~8mm, outer diameters of ~9.5mm, and in length up to approximately one meter.

Lengths of cladding tubes were subsequently sealed by bonding monolithic CVD SiC endplugs to the ends of the tubes using the GA HSiC joining process. This process is a hybrid approach where a SiC polymer precursor based slurry was pyrolyzed and then infiltrated using SiC CVI to form a high purity SiC-based joint, and has been described in more detail in the literature [3]. Examples of open-ended and sealed cladding tubes are shown in Fig. 1. The fabrication of some samples containing interior components (such as fuel pellets or retaining clips or springs) required use of an adapted joining method which used local heating to minimize thermal effects on components located away from the end of the tube where the joining and sealing process was carried out.

Fig. 1: (left) examples of open and closed end SiC-based cladding tubes, and (right) magnified view of SiC-cladding tube sealed with a SiC endplug and HSiC joint

2.2. Mechanical Testing

High temperature C-ring testing was performed using the guidance and equations provided in ASTM C1323-16 [6] and Jacobsen et al [4]. Nominal specimen widths were 2-2.5 mm and a

minimum of 5 specimens were tested at each temperature. Testing was performed using an Instron universal mechanical test frame with an integrated Centorr sealed chamber vacuum furnace. Test hardware was made from high strength graphite rod. Testing was performed under gently flowing Argon at a crosshead rate of 2 mm/min.

High temperature expanding plug testing was performed using guidance and equations provided in ASTM C1819-15 [7] and Chuck et al [8]. The expanding plug material used for the room temperature tests is 95A durometer polyurethane from McMaster-Carr which has been used in previous work by GA [4]. For high temperature tests, a 99.95% pure niobium metal was used as the expanding plug material. Monolithic CVD SiC push rods were used for test fixturing. To account for the loads required to compress the plug material, for both room temperature and high temperature tests, the plugs were compressed without the sample confinement, referred to as a blank test, are then subtracted from the loads measured during sample tests. A minimum of 4 specimens were tested at each temperature.

In high temperature testing, samples were typically heated at rates of 15 °C per minute, and samples were held at the test temperature for 30 to 60 minutes before loading was applied.

2.3. Thermal Analysis

In this work, thermal conductivity of SiC-based cladding tubes was measured in the through-thickness direction. Thermal diffusivity was measured using a NETZSCH LFA 427 laser flash analyzer, and this value, along with cladding sample density and specific heat was used to calculate the thermal conductivity. In order to account for the impact of the tube curvature on the measurement, a correction was included using an approach detailed in the literature [9].

2.4. Leak Testing

Leak rate testing was performed using an Agilent VS MD30 Helium Leak Detector, which is sensitive to helium leak rates up to 5e-12 atm*mL/sec. For open ended tubes, one end is bonded to a stainless steel blank disk by epoxy while the other end is epoxy bonded to a vacuum flange fixture with a through hole that is directly connected to the leak detector as shown in Fig. 2a. A through-hole in the vacuum flange allows any helium passing through the test material to enter the helium leak detector (HLD). The epoxy has been tested for permeation and was found to have negligible leak rates. For rodlets which have already been processed to have one end sealed, then open end is bonded to a vacuum flange using a similar epoxy approach as open ended tubes, and this allowed leak rate measurements to be obtained for the combination of the cladding tube with one end sealed.

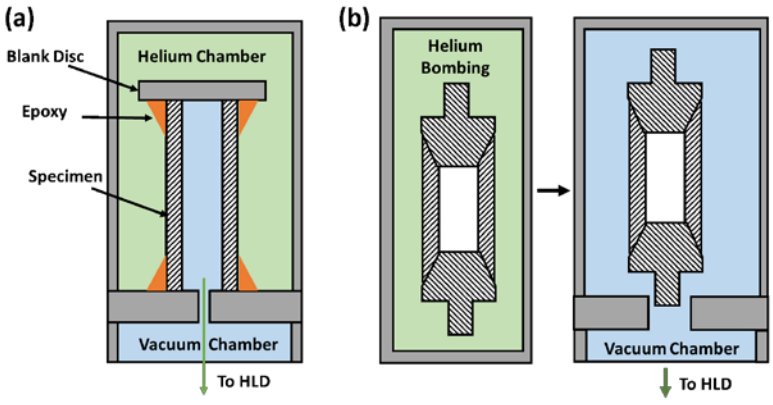

Fig. 2: (a) Helium Leak Check Setup, and (b) Helium Bombing Test Setup

After fully sealing the rodlets by joining endplugs to both ends, the leak test method as described above could no longer be performed; instead, GA uses a test method adapted from fully sealed metal fuel rods. The rodlets were pressurized to 3.8 MPa (550 psig) of helium for

10 minutes in a helium bomb chamber in order to fill the specimen with helium through any potential leak paths. To minimize helium outgassing during leak measurements, the specimens were then moved to a different test chamber and then connected to the VS MD30 leak detector within 5 minutes in order to measure the leak rate of helium escaping the rodlet. The schematic of the test setup is shown in Fig. 2b. It should be noted that the surface outgassing after the helium bombing step is expected, therefore leak rates were measured for several hours.

2.5. Corrosion Testing

Corrosion testing was done using a flowing loop autoclave at the Westinghouse Churchill laboratory facility. The autoclave pressure was 18.6 MPa and the temperature was 343 °C during the exposures, which ranges from approximately five to twenty days per run. The water chemistry was controlled to a simulated PWR coolant chemistry, with boron and lithium concentrations typical of LWR in the middle of a cycle, with a dissolved hydrogen concentration of ~50 mL(STP)/kg water, and with dissolved oxygen concentration of < 3 ppb. At the conclusion of each run, the samples were carefully dried and weighed, and samples were subjected to multiple runs to accumulated total cumulative exposures of up to ~150 days.

3. Results and Discussion

In order to demonstrate and engineered SiC-SiC cladding with enhanced accident performance, testing must show behavior that not only satisfies normal operational requirements, but also offers superior response during simulated accident conditions. Several recent publications have simulated stresses for SiC-SiC cladding during normal operation [5] [10], and these can inform strengths needed during normal operation. In addition to strong mechanical performance, cladding must also be made with high thermal conductivity and cladding, endplugs, and joints must be made leak-tight. Cladding must also survive exposure to corrosion coolant chemistries, which can be tested inside loop positions in test reactors or in autoclaves to simulate temperature, pressure, and chemistry conditions. Beyond performance during normal operation, the enhanced accident tolerance of SiC-SiC cladding must also be measured, and one route to assess this is to show strength retention to extremely high temperatures. Recent progress in the demonstration of engineered SiC-SiC cladding performance in these areas is summarized below.

3.1. Mechanical Performance

In order to define the benefits SiC-based cladding brings to utilities, it is necessary to understand the mechanical performance of the cladding in accident conditions. This data is also needed to help understand failure modes for modeling purposes, as ceramic composite mechanical behavior, especially at high temperatures, differs in significant ways from their metals based counterparts. To begin to define this behavior GA has performed C-ring testing and expanding plug testing at temperatures up to 1900 °C.

Results of high temperature C-ring testing in argon can be seen in Fig. 3. No significant drop in strength versus room temperature results are observed over the range of test temperatures which cover temperatures from normal operating conditions to temperatures that may be anticipated in LOCA type events. The relatively large observed standard deviations are mainly due to uncertainty associated with compression of the furnace bellows relatively to the relatively low loads measured during C-ring testing and is not believed to be representative of sample variation. The maximum test temperature of the equipment was reached before seeing any significant drop in strength. This is in contrast to Zircaloy, which shows greater than 75% loss of room temperature strength at temperatures as low as 800 °C [11]. Additional information on this testing can be found in Shapovalov et al. [12].

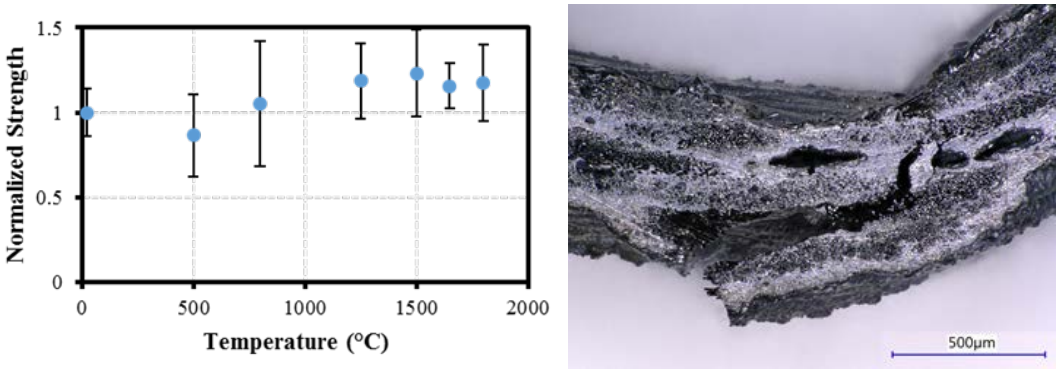

Fig. 3: (left) Strength as a function of temperature for high temperature C-Ring testing in argon, and (right) Micrograph of C-Ring failure location after testing at 1500 °C

Failure modes during C-ring testing are consistent with SiC based composite materials. Evidence of both crack deflection and fiber pullout is observed up to 1650 °C, Figure 3, which are both considered strong indicators of improved fracture toughness due to continuous fiber reinforcement. At the maximum test temperature (>1800 °C), a more brittle like fracture behavior was observed, which is attributed to the microstructural changes in both the matrix (initial beginnings of β to α phase transformation) [13] as well as crystallization and grain growth in the fibers [2]. The observed brittle fracture did not appear to affect the overall failure strength of the material.

While C-ring testing is a fast, easy to implement, high temperature test technique, a mixed mode bending stress is present that can complicate interpretation of results and there is a large benefit to performing testing more representative of pellet cladding mechanical interactions expected in accident conditions. To better replicate this stress state, expanding plug testing was used where a hoop tensile dominate stress state is present. Niobium was chosen as an expanding plug material due to its high melting point, its relative softness at test temperature, a high Poisson's ratio (for metal), and its lack of apparent reactivity with SiC at test temperatures.

Normalized ultimate hoop strength as a function of temperature determined by the expanding plug test is shown in Fig. 4. Similar to C-ring testing, full retention of room temperature strength is observed to at least 1650 °C. However, tests done at ~1900 °C showed a reduction in strength. There is evidence that the reduction in strength is due to the phase transformation and grain growth discussed earlier. It is interesting that this drop off was not observed in C-ring testing, and additional testing is underway to better understand this phenomenon. Additional testing of "harder" surrogate fuel pellets that may better represent ceramic or metallo-ceramic fuels like doped UO_2 or U_3Si_2 is also being planned.

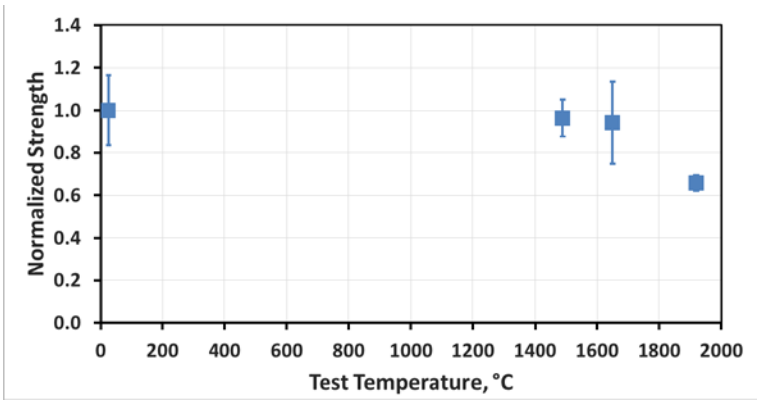

Fig. 4: Ultimate strength at high temperatures determined by expanding plug test

Images of the main fracture sites are shown in Fig. 5. In all tests the largest crack is oriented along the axis of the tube indicating a failure predominantly due to hoop direction loading. At room temperature and at 1490 °C the main crack is deflected to circumferential cracks indicating the boundaries of the pressurized area on the ID of the test specimens, as the plug is undersized relative to the total tube length. Fracture at 1920 °C shows shorter crack paths with minimal monolithic layer delamination. This change in behavior is attributed to some loss of ductility as well as changes in plug properties at higher temperatures. All samples exhibited a graceful failure behavior by maintaining a tubular geometry with minimal ballooning or fracturing into pieces, even at very high test temperatures.

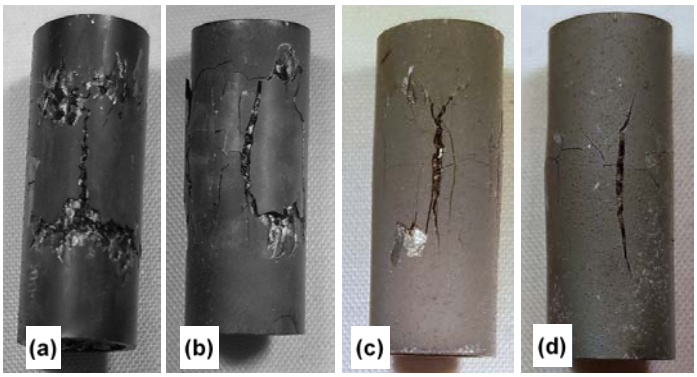

Fig. 5: a) Typical crack pattern for an expanding plug test (a) at room temperature, at (b) at 1490 °C, (c) at 1650 °C, and (d) at 1920 °C

3.2. Thermal Properties

Thermal conductivity is a key performance parameter for SiC-based fuel cladding, as irradiation-induced reductions in thermal conductivity can lead to high through-thickness temperature gradients and corresponding stresses. Recent thermal conductivity measurements on SiGA cladding specimens fabricated at General Atomics show that SiC-based multi-layered engineered cladding can be reliably produced with room temperature thermal conductivities between 18 and 28 W/m-K (Fig. 6). These thermal conductivity values were calculated using a laser-flash analysis thermal diffusivity measurement of curved sections of cladding tubes, and a correction for the tube curvature was applied using the method described by Zhang et al [9]. During testing, each sample was measured three times at each temperature, and each data point plotted represented the average of measurements from at least three samples from each batch. The thermal conductivity values measured in this work for Hi-Nicalon Type-S CVI composite cladding samples are larger than previously reported values for planar samples [2]. This enhancement is attributed to improved densification of the composite structure during fabrication and the inclusion of a monolithic SiC layer on the outer surface of the engineered cladding.

In addition to the consistent, large room temperature values, Fig. 6 shows distinct variation between batches that is persistent over the entire sampled temperature regime. Samples from batches with higher density exhibit better thermal conductivity. This largely explains the intra-batch variations ($\rho_{Batch\,A} < \rho_{Batch\,B} < \rho_{Batch\,C}$). The thickness of the outer monolithic layer (and the relative fraction of the monolithic SiC layer thickness to the overall wall thickness) can have a large contribution to the thermal conductivity, as the monolithic layer is both denser (near full theoretical density of 3.2g/cm^3), and the thermal conductivity of monolithic CVD SiC can be substantially higher (~70-300 W/m-K) [14]. As a result, high-conductivity SiC-based cladding material can be produced through control of both the infiltration (targeting high composite layer density), and the engineered cladding structure (gaining both density and thermal conductivity improvements from the outer monolithic layer).

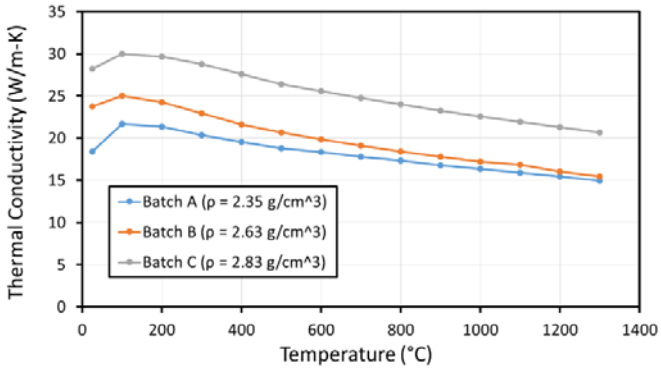

Fig. 6: Plot of thermal conductivity vs. temperature for SiGA cladding material produced in batches with three different densities

Reliable production of cladding with strong thermal properties is essential, as the thermal conductivity of SiC-based cladding is a key constraint for ATF cladding design. A recent study [15] has suggested that a SiC based cladding featuring a thermal conductivity above 12 W/m-K will lead to the same or lower cladding/fuel temperatures when compared to Zr4 cladding under normal operating conditions. General Atomics has demonstrated strong thermal conductivity of SiGA cladding through continued refinement of the fabrication process, and further reduction of inter and intra-batch consistency is being pursued through careful control of the SiC outer monolithic layer. The thermal conductivity of SiC is known to degrade under irradiation [2], and the thermal conductivity of cladding samples irradiated under representative LWR conditions is also very important to understand. Irradiation testing and subsequent PIE is being planned to investigate these irradiation effects.

3.3. Hermeticity

Leak rate measurements are taken at various stages of the cladding fabrication process to verify that the SiC-based cladding is hermetic and to ensure there are no major changes in hermeticity during processing. Baseline measurements were made on GA's SiC-SiC composite tubes before any end plug joining, and samples were measured again following completion of the HSiC joint for the first endplug in each tube. The fabrication of hermetic SiC-based cladding tubes and endplug joints can be reliably achieved, and for tubes measured with one end sealed, more than 80% of samples achieved a leak rate of 1E-8 atm*mL/sec or better, as shown in Fig. 7.

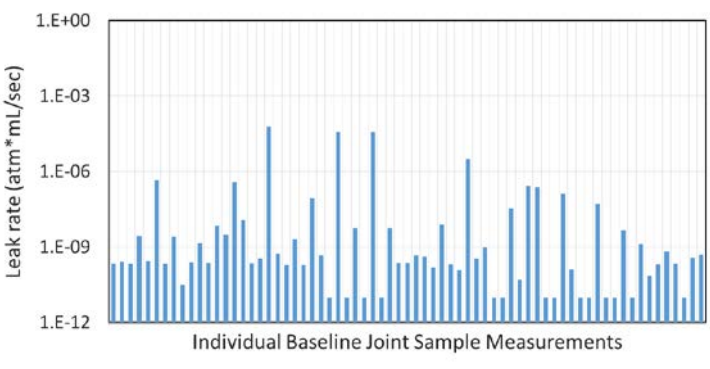

Fig. 7: Leak rate measurements obtained for individual tube samples with one end sealed

Once the cladding tube and the first endplug joint has been verified to meet leak rate specifications, samples can be loaded as needed for testing purposes, and the second end of the tube can be sealed. A modified HSiC joining process that utilizes local heating is used for this process, and several rodlets samples (>300mm in length) have been fabricated to demonstrate manufacturability. The modified joining method, together with the cladding

fabrication and joining process for the first end, results in sealed samples with a high purity, CVD SiC coating over the entire exterior, to provide both a hermetic barrier to fission gases and to provide improved corrosion resistance. This modified joining approach can also be used to incorporate a gas backfill (such as helium, to offer improved pellet-cladding gap thermal conductance).

Leak rate for two representative specimens at various fabrications stages can be seen in Tab. 1. The final leak rate for fully sealed rodlets can be found over a 2 hour period (to allow sufficient time for out-gassing) at 2.2E-8 and 3.0E-8 atm*mL/sec, which matches up with current leak rate requirements, derived from full length Zircaloy metal cladding.

Sample #	Tube Only	Post Endplug Joining	Final Sealed and Coated Rodlet
Sample 1	~5.5E-10	6.34E-10	2.19E-8
Sample 2	~5.5E-10	4.90E-10	2.98E-8

*Tab. 1: Leak Rates at various fabrication stages for two fully sealed and pressurized rodlets (units are in atm*mL/sec)*

These results demonstrate the fabrication of a fully sealed, pressurized, SiC-SiC composite rodlet. The rodlet remains hermetic throughout all processing steps with very little degradation in all but the final CVD top coat step.

3.4. Corrosion Testing

Short (~50mm long) SiC-cladding samples which were sealed with endplugs joined at both ends using the HSiC joining process were subjected to a sequence of autoclave exposures under the conditions described in section 2.5. One particular set of three sealed samples has been exposed to nearly 150 days of total autoclave exposure, with multiple intervals where exposure was stopped, the samples were removed, cleaned, dried, and weighed, and then testing resumed using the same samples. Results for the mass loss normalized to sample surface area are shown in Figure 5. It was observed that corrosion behavior can be highly dependent on fabrication processing conditions, especially CVD SiC deposition conditions and joint processing conditions. For example, samples with CVD SiC deposited at lower temperatures, and samples with transient eutectic phase (TEP) processed SiC did not perform as well as the samples shown in Fig. 8 [16].

This data can be compared against corrosion specifications. Allowable corrosion must not compromise cladding performance or retention of hermeticity, and must not exceed dissolved silica limits. The specifications defined by these limits will vary depending on the intended use of test samples, and the number of samples, and Westinghouse has previously calculated allowable specifications for test reactor irradiations, for Lead Test Assembly (LTA) irradiations, and for full cores of fuel utilizing SiC-based cladding [17].

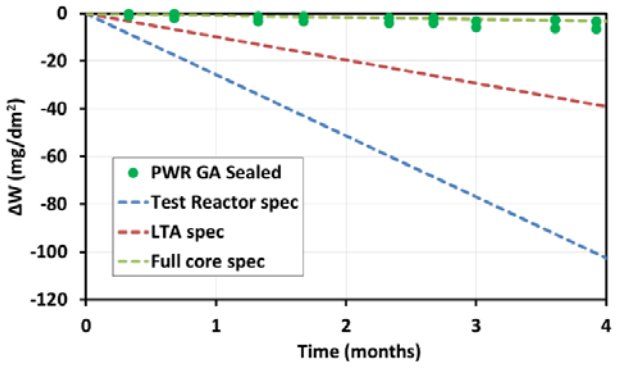

Fig. 8: Average mass loss normalized to surface area for a set of three sealed SiC-cladding rodlets compared to corrosion rate specifications calculated by Westinghouse [17]

These results show that a fully SiC-based cladding sample with ends sealed using a HSiC joining method can provide acceptable corrosion results based on autoclave testing. The corrosion data from these samples meets both test reactor irradiation specifications an LTA specifications, and is very close to required specifications for full cores of SiC-cladding accident tolerant fuel. Further refinement and improved repeatability of the cladding and joining fabrication processes are in progress to ensure full core specifications will be reliably met. Ongoing testing at the MIT reactor is focusing on showing that similar excellent corrosion performance can be obtained under a combination of exposure to PWR chemistry with neutron irradiation. Additional recent results for both in-reactor and autoclave testing are provided by Xu et al [16].

4. Conclusions

Recent developmental efforts have shown excellent SiC-based cladding performance in the areas of high temperature mechanical strength, high thermal conductivity, leak tightness, and corrosion resistance. Samples of engineered, multi-layered SiGA cladding were fabricated with well controlled dimensions and surface roughness for testing in both open-ended and sealed geometries. Open-ended samples were subjected to mechanical testing in the hoop direction at temperatures up to 1920 °C, and showed full strength retention to 1650 °C and retention of a coolable, tubular geometry for all temperatures examined. The engineered cladding showed as-fabricated thermal conductivity up to ~30 W/m-K. This data is as high as or higher than other data on CVI-fabricated SiC-SiC composites in the literature, and increased thermal conductivity will result in lower temperature gradient-induced stresses during operation. Recent fabrication advances have produced cladding tubes and endplug joints that can meet challenging hermeticity requirements with a high yield of samples achieving helium leak rates measured at 1E-8 atm*mL/sec or better. For sealed samples fabricated under well-controlled conditions, corrosion measured in autoclave exposure under PWR water chemistry is very low, and meets requirements defined for test reactor irradiations and lead test rod and lead test assembly irradiations.

Development work on SiGA cladding is ongoing, with upcoming work focusing on continued manufacturing refinements and scale-up, confirmation of cladding and joint strength, gas tightness, and corrosion performance under irradiation, and fabrication and irradiation of fueled rodlets. These efforts are on track and on schedule to support fabrication of lead test rods with a planned 2022 insertion.

5. Acknowledgements

This work was supported by GA IR&D funding and the Department of Energy under Award Number DE-NE0008222. This report was prepared as an account of work sponsored by an agency of the United States Government. Neither the United States Government nor any agency thereof, nor any of their employees, makes any warranty, express or implied, or assumes any Sub-recipient liability or responsibility for the accuracy, completeness, or usefulness of any information, apparatus, product, or process disclosed, or represents its use would not infringe privately owned rights. Reference herein to any specific commercial product, process, or service by trade name, trademark, manufacturer, or otherwise, does not necessarily constitute or imply its endorsement, recommendation, or favoring by the United States Government or any agency thereof. The views and opinions of authors expressed herein do not necessarily state or reflect those of the United States Government or any agency thereof.

6. References

[1] C. P. Deck, G. M. Jacobsen, J. Sheeder, O. Gutierrez, J. Zhang, J. Stone, H. E. Khalifa and C. A. Back, "Characterization of SiC-SiC composites for accident tolerant fuel cladding," Journal of Nuclear Materials, vol. 466, pp. 667-681, 2015.

[2] Y. Katoh, K. Ozawa, C. Shih, T. Nozawa, R. J. Shinavski, A. Hasegawa and L. L. Snead, "Continuous SiC fiber, CVI SiC matrix composites for nuclear applications: Properties and irradiation effects," Journal of Nuclear Materials, vol. 448, pp. 448-476, 2014.
[3] H. E. Khalifa, C. P. Deck, O. Gutierrez, G. M. Jacobsen and C. A. Back, "Fabrication and characterization of joined silicon carbide cylindrical components for nuclear applications," Journal of Nuclear Materials, vol. 457, pp. 227-240, 2015.
[4] G. M. Jacobsen, J. D. Stone, H. E. Khalifa, C. P. Deck and C. A. Back, "Investigation of the C-ring test for measuring hoop tensile strength of nuclear grade composites," Journal of Nuclear Materials, vol. 452, pp. 125-132, 2014.
[5] J. G. Stone, R. Schleicher, C. P. Deck, G. M. Jacobsen, H. E. Khalifa and C. A. Back, "Stress Analysis and Probabilistic Assessment of Multi-layer SiC-based Nuclear Fuel Cladding," Journal of Nuclear Materials, vol. 466, pp. 682-697, 2015.
[6] ASTM C1323: Standard Test Method for Ultimate Strength of Advanced Ceramics with Diametrally Compressed C-Ring Specimens at Ambient Temperature, West Conshohocken, PA: ASTM International, 2010.
[7] ASTM C1819: Standard Test Method for Hoop Tensile Strength of Continuous Fiber-Reinforced Advanced Ceramic Composite Tubular Test Specimens at Ambient Temperature Using Elastomeric Inserts, West Conshohocken: ASTM International, 2015.
[8] L. Chuck, S. Goodrich and C. Barklay, "A Review of Hydraulically Pressurized Ceramic Tube Test for Hoop Tensile Strength from Ambient to Elevated Temperatures at UDRI," in Int'l Conf & Expo on Advanced Ceramics and Composites, Daytona Beach, FL, 2016.
[9] J. Zhang, H. E. Khalifa, C. P. Deck, J. Sheeder and C. A. Back, "Thermal diffusivity measurement of curved samples using the flash method," in Proceedings of the 39th Int'l Conf & Expo on Advanced Ceramics & Composites, Daytona Beach, FL, 2015.
[10] M. Ben-Belgacem, V. Richet, K. A. Terrani, Y. Katoh and L. L. Snead, "Thermo-mechanical analysis of LWR SiC/SiC composite cladding," Journal of Nuclear Materials, vol. 447, pp. 125-142, 2014.
[11] K. J. Geelhood, C. E. Beyer and W. G. Luscher, "PNNL-17700: PNNL Stress/Strain Correlation for Zircaloy," U.S. Department of Energy, Pacific Northwest National Labratory, 2008.
[12] K. Shapovalov, G. M. Jacobsen and C. P. Deck, "Mechanical Response of SiC-SiC Composite Cladding at Accident Relevant Temperatures," in American Nuclear Society Annual Meeting, American Nuclear Society, Philadelphia, PA, 2018.
[13] G. M. Jacobsen, K. Shapovalov, E. Song and C. P. Deck, "Mechanical Behavior of Nuclear Grade SiC-SiC Tubing at Operating and Accident Temperatures," in Pacific Rim Conference on Ceramic and Glass Technology, Waikoloa, HI, 2017.
[14] L. Snead, T. Nozawa, Y. Katoh, T.-S. Byun, S. Kondo and D. A. Petti, "Handbook of SiC properties for fuel performance modeling," Journal of Nuclear Materials, vol. 371, pp. 329-377, 2007.
[15] C. Cozzo and S. Rahman, "SiC cladding thermal conductivity requirements for normal operation and LOCA conditions," Progress in Nuclear Energy, vol. 106, pp. 278-283, 2018.
[16] P. Xu, E. J. Lahoda, J. Lyons, C. P. Deck and G. E. Kohse, "Status Update On Westinghouse Sic Composite Cladding Fuel Development (Paper # A0105)," in 2018 Water Reactor Fuel Performance Meeting, Prague, Czech Republic, 2018.
[17] P. Xu , E. Lahoda, R. Jacko, F. Boylan and R. Oelrich, "Status of Westinghouse SiC Composite Cladding Fuel Development (Paper A0184)," in Water Reactor Fuel Performance Meeting (WRFPM), Jeju Island, South Korea, 2017.